

Bound states of edge dislocations: The quantum dipole problem in two dimensions

K. Dasbiswas, D. Goswami, C.-D. Yoo, and Alan T. Dorsey

Department of Physics, University of Florida, P.O. Box 118440, Gainesville, Florida 32611-8440, USA

(Received 18 December 2009; revised manuscript received 1 February 2010; published 25 February 2010)

We investigate bound-state solutions of the two-dimensional Schrödinger equation with a dipole potential originating from the elastic effects of a single edge dislocation. The knowledge of these states could be useful for understanding a wide variety of physical systems, including superfluid behavior along dislocations in solid ^4He . We present a review of the results obtained by previous workers together with an improved variational estimate of the ground-state energy. We then numerically solve the eigenvalue problem and calculate the energy spectrum. In our dimensionless units, we find a ground-state energy of -0.139 , which is lower than any previous estimate. We also make successful contact with the behavior of the energy spectrum as derived from semiclassical considerations.

DOI: [10.1103/PhysRevB.81.064516](https://doi.org/10.1103/PhysRevB.81.064516)

PACS number(s): 67.80.B-, 02.60.-x

I. INTRODUCTION

There has been broad interest over the years in the physics of solids containing dislocations. In addition to affecting the mechanical properties of solids, the strain field associated with dislocations binds charge carriers in metals, or solute impurities in a generic solid.¹ As such, the presence of dislocations has a significant effect on the transport, elastic, and superconducting properties of the solid. In this context, it is important to know the spectrum of localized states due to a dislocation.

In this paper, we discuss the spectrum of bound states for an edge dislocation. Within linear elasticity theory the deformation potential due to an edge dislocation is proportional to the stress tensor or the divergence of the elastic displacement field. Considering a straight edge dislocation, oriented along the z axis, within a continuum model, this potential is given by

$$V(r, \theta) = p \frac{\cos \theta}{r}, \quad (1)$$

where p is the strength of the “dipole” potential, r is the distance from the dislocation axis, and θ is the azimuthal angle, both defined in the x - y plane.¹ The dipole moment p depends on quantities such as the Fermi energy and the lattice and elastic constants of the solid. In an electrostatics context this potential can be realized as a dipole built by bringing two infinite line charges of opposite sign close together. Here we address the quantum dipole problem by considering the solution of the corresponding two-dimensional (2D) Schrödinger equation,

$$-\frac{\hbar^2}{2m} \nabla^2 \psi + p \frac{\cos \theta}{r} \psi = E \psi. \quad (2)$$

For $p > 0$ this potential is attractive for $x < 0$ (thus, allowing for bound states) and repulsive for $x > 0$. It has parity in y ; i.e., symmetry on reflection about the x axis, which should be reflected in the eigenfunctions as well. The solution of the Schrödinger equation is complicated due to the noncentral nature of the potential.² The potential being nonseparable further impairs the applicability of the WKB approximation.

We are particularly motivated by the supersolid problem,³ and a possible interpretation of it which considers superfluidity to exist not in the bulk of solid ^4He but along a network of dislocations.⁴ We would like to solve the full nonlinear Ginzburg-Landau (GL) theory for such a system, for which we would first need to know the solution of the linearized equation. The lowest eigenvalue of the linear equation is actually a measure of the local enhancement in T_c produced by a dislocation. Further, the solution of the linear GL theory can be used to affect a separation of the transverse degrees of freedom in the full nonlinear time-dependent GL equation, resulting in a one-dimensional “amplitude equation” of superfluid density along the dislocation. The effective dimensionless coupling constant of this one-dimensional theory is $g = \int dx dy |\phi_0(x, y)|^4$, where $\phi_0(x, y)$ the normalized ground-state eigenfunction of the linear GL equation. Our numerical solution of the linear equation allows us to calculate this parameter which acts as an input to the weakly nonlinear analysis.⁵

The problem of finding the ground-state energy of the quantum dipole problem has a long history, starting from the work of Landauer in 1954,⁶ who used a variational approach. Subsequent authors used a variety of techniques for this estimate: semiclassical⁷ or purely variational^{8,9} methods, a combination of variational and perturbative methods¹⁰ or an expansion in terms of known basis functions,^{11,12} but to solve this we have used a direct numerical method. Some prior works^{9,10} have also studied the spectrum of the bound eigenstates. The ground-state energies calculated in these works are shown in Table I, together with the numerical value obtained in this paper.

In the next section, we provide the details of our variational calculation for the ground-state energy, including our choice of a suitable trial wave function. Next, we discuss the results and technical details of the several numerical methods we have used to calculate the eigenvalue spectrum, and their relative merits and disadvantages. The methods involve diagonalization of the Hamiltonian, carried out both in real space and in the basis of two-dimensional hydrogenic wave functions (in contrast with previous calculations with different choices of basis expansions, e.g., Refs. 11 and 12). Here we also compare the results obtained using different meth-

TABLE I. Summary of ground-state energy estimates of the edge-dislocation potential. Energy is given in units of $2mp^2/\hbar^2$.

References	Ground state estimate
Landauer (1954) ^a	-0.102
Emtage (1967) ^b	-0.117
Nabutovskii and Shapiro (1977) ^c	-0.1014
Slyusarev and Chishko (1984) ^d	-0.1111
Dubrovskii (1997) ^e	-0.1196
Farvacque and Francois (2001) ^f	-0.1113
Dorsey and Toner ^g	-0.1199
This work	-0.139

^aReference 6.

^cReference 10.

^bReference 8.

^fReference 12.

^eReference 11.

^gReference 13.

^dReference 9.

ods, which are found to agree in the essential features. In the final section, we provide a semiclassical argument to justify our results together with some discussion of the interesting properties of the classical problem. The semiclassical result is found to extend to the lower-energy eigenstates as well.

II. VARIATIONAL CALCULATION

Our initial approach to determine the ground-state energy has been variational because this can be carried out analytically and provides a rough estimate which can then guide our more explicit numerical solution. Given a normalized wave function $\psi(r, \theta)$, we minimized the energy functional,

$$F[\psi, \psi^*] = \int d^2x \left(\frac{\hbar^2}{2m} |\nabla \psi|^2 + p \frac{\cos \theta}{r} |\psi|^2 \right). \quad (3)$$

This functional has its extrema at the solutions of the Schrödinger equation, Eq. (2). Note that the length and energy scales which emerge from Eq. (3) (or the Schrödinger equation) for this problem are $\hbar^2/2mp$ and $2mp^2/\hbar^2$. In dimensionless variables, the normalized trial wave function used in our calculation is

$$\psi(r, \theta) = \frac{2AB}{C\sqrt{\pi}} \frac{(1-r/BC)}{\sqrt{(3-4B+2B^2)}} \exp\left(-\frac{r}{C}\right) - \frac{\sqrt{1-A^2}}{C^2} \sqrt{\frac{8}{3\pi}} r \cos \theta \exp\left(-\frac{r}{C}\right), \quad (4)$$

where A , B , and C are variational parameters. We choose the trial wave function so as to account for the anisotropy of the potential. Further, the asymptotic behavior of the potential is captured by the exponentially decaying factors. The minimum expectation value of the energy occurs when $A=0.803$, $B=-0.774$, and $C=2.14$ with a ground-state energy of -0.1199 which was found by Dorsey and Toner.¹³ This value is 2.5% lower than the previous lowest variational estimate (-0.1196) obtained by Dubrovskii.¹⁰ In addition, by

using this normalized trial wave function as the $\phi_0(x, y)$ we find the parameter $g = \int dx dy |\phi_0(x, y)|^4 = 0.017$.

III. NUMERICAL METHODS

A detailed numerical solution of the two-dimensional Schrödinger equation with the dipole potential, Eq. (2), is likely to provide more accurate ground-state eigenvalues in addition to determining the rest of the bound-state eigenvalues and corresponding wave functions. We do this both by a real-space diagonalization, where the Schrödinger equation is discretized on a square grid, and by expanding in the basis of the eigenfunctions of the two-dimensional Coulomb potential problem. Two special features of this dipole potential make it a numerically difficult problem: the singularity at the origin and the long-range behavior of the potential. It is expected that the Coulomb wave functions would be better suited to capturing this long-range behavior and convergence would consequently be faster. Our results show that the Coulomb basis method is more accurate for the higher bound states (which are expected to extend more in space), as the real-space methods are limited by size issues. However, the real-space method works better for the ground state.

A. Real-space diagonalization method

For numerical purposes the Schrödinger equation is converted to a difference equation on a square grid of spacing h , with the Laplacian approximated by its five-point finite-difference form,¹⁴ resulting in a block tridiagonal matrix of size $N^2 \times N^2$, where the grid has dimensions of $N \times N$. Each diagonal element corresponds to a grid point and has values of $4/h^2 + V(x, y)$, whereas the nonzero off-diagonal elements all equal $-1/h^2$. The matrix is thus very large but sparse. We use three different numerical methods to diagonalize this matrix: the biconjugate gradient method,¹⁵ the Jacobi-Davidson algorithm,¹⁶ and Arnoldi-Lanczos algorithm,¹⁷ with the latter two being more suited to large sparse matrices whose extreme eigenvalues are required. We use freely available open source packages [JADAMILU (Ref. 18) and ARPACK (Ref. 19)] written in FORTRAN for both. All three approaches are projective Krylov subspace methods, which rely on repeated matrix-vector multiplications while searching for approximations to the required eigenvector in a subspace of increasing dimensions. Reference 20 provides a concise introduction to the Jacobi-Davidson method, together with comparisons to other similar methods. The implicitly restarted Arnoldi package (ARPACK) is described in great detail in Ref. 21. Some general issues about the real-space diagonalization as well as some specific features of the three methods used for it are discussed below.

The accuracy of the real-space diagonalization methods is controlled by two main parameters: the grid spacing h and the total size of the grid, which is given by Nh . The finite-difference approximation together with the rapid variation in the potential near the origin imply that the solution of the partial differential equation would be more accurate for a smaller grid spacing. We work with open boundary conditions, which means that a bound-state wave function could

be correctly captured only if the total size of the grid were to be greater than the natural decay length of the wave function. In other words, the eigenstate has to be given enough space to relax. This limits the number of bound states we can calculate accurately because a large grid size together with small grid spacings calls for a large number of grid points, thus quadratically increasing the size of the matrix to be diagonalized. Computational resources as well as the limitations of the algorithms themselves place an effective upper bound on the size of a diagonalizable matrix. We experimented to find that a $10^6 \times 10^6$ size sparse matrix was about the maximum that could be diagonalized with our computational resources.

The origin of the square grid is symmetrically offset in both x and y directions to avoid the $1/r$ singularity. We first tested the accuracy of the real-space techniques for the case of the two-dimensional Coulomb potential, the spectrum of which is completely known.²² We observe that for various lattice sizes the biconjugate method captures at most the first four states whereas the Jacobi-Davidson method returns 20 eigenstates. The eigenvalues obtained from both methods are accurate to within 2% of the exact values.²²

We have applied the biconjugate method to the edge-dislocation potential for various lattice sizes, varying from 10×10 to 600×600 . The number of eigenstates captured increases with the size of the lattice, as expected. The ground-state energy is observed to vary from -0.134 to -0.142 . We also observe that for the number of grid points exceeding $N=2000$ we encounter a numerical instability due to the accumulation of round-off errors. For the largest real-space grid size of 600×600 ($N=1200$, $h=0.5$) we obtain seven eigenstates with a ground-state energy of -0.139 .

The ground-state energy from the Jacobi-Davidson method, employed for the same lattice size gives -0.139 , which matches well with our expectations from the variational calculation. We are able to obtain 20 bound-state eigenvalues in this method using $N=1000$, $h=0.5$. It is checked that the low-lying eigenvalues are not very sensitive to values of h in this regime, so a relatively large value of 0.5 serves our purpose. As pointed out earlier, the accuracy of this method is determined by the choice of lattice parameters. The variation in the calculated ground-state eigenvalue for differing lattice parameters is within 0.001, which therefore is the estimated error in the calculation of eigenvalue.

The Arnoldi-Lanczos method yields the same eigenvalues to within estimated error. It takes more time and memory resources to converge but can calculate more eigenvalues. It provides 30 bound-state eigenvalues for the same set of lattice parameters as the above. Finally, after calculating the ground-state wave function we find that the coupling constant $g=0.0194$, slightly larger than the variational estimate of $g=0.017$.

B. Coulomb basis method

We also calculate the spectrum numerically by using the linear variational method with the basis of the 2D hydrogen atom wave functions.²² There are two advantages of this method over the real-space diagonalization methods. First,

the linear variational method is capable of capturing more excited states because the number of calculated bound states is not limited by the size of the real-space grid but by the number of long-range basis functions. Second, the singularity at the origin of the edge-dislocation potential does not pose a problem anymore because elements of the Hamiltonian matrix become integrable.

Now we calculate the elements of the Hamiltonian matrix with a 2D edge-dislocation potential. The Schrödinger equation with the 2D Coulomb potential is analytically worked out in Ref. 22. The normalized wave functions of a 2D hydrogen atom are given by

$$\psi_{n,l}^H(r, \theta) = \sqrt{\frac{1}{\pi}} R_{n,l}(r) \times \begin{cases} \cos(l\theta) & \text{for } 1 \leq l \leq n \\ \frac{1}{\sqrt{2}} & \text{for } l = 0 \\ \sin(l\theta) & \text{for } -n \leq l \leq -1, \end{cases} \quad (5)$$

where

$$R_{n,l}(r) = \frac{\beta_n}{(2|l|)!} \sqrt{\frac{(n+|l|-1)!}{(2n-1)(n-|l|-1)!}} (\beta_n r)^{|l|} \times \exp\left(-\frac{\beta_n r}{2}\right) {}_1F_1(-n+|l|+1, 2|l|+1, \beta_n r), \quad (6)$$

with $\beta_n = 2/(2n-1)$ and ${}_1F_1$ being the confluent hypergeometric function. The elements of the Hamiltonian with the 2D dipole potential are

$$\langle \psi_{n_1, l_1}^H | -\nabla^2 | \psi_{n_2, l_2}^H \rangle = \delta_{l_1, l_2} \int_0^\infty dr \left(1 - \frac{\beta_{n_2}^2}{4} r \right) \times R_{n_1, l_1}(r) R_{n_2, l_2}(r), \quad (7)$$

$$\langle \psi_{n_1, l_1}^H | \frac{\cos \theta}{r} | \psi_{n_2, l_2}^H \rangle = \tilde{V} \int_0^\infty dr R_{n_1, l_1}(r) R_{n_2, l_2}(r), \quad (8)$$

where $\tilde{V} = \delta_{l_1, l_2 \pm 1} / 2$ if both l_1 and l_2 are less or greater than 0, or $\tilde{V} = 1/\sqrt{2}$ if l_1 is 0 and l_2 positive or vice versa. The spectra are obtained for several total numbers of basis functions N_{basis} . Due to the numerical precision in calculating elements of the Hamiltonian matrix N_{basis} cannot be increased to more than 400. For $N_{\text{basis}}=400$ we obtain about 150 bound states and the ground-state energy of -0.0969 . This calculated ground-state energy is not reliable as it is higher than even the upper bound of -0.1199 estimated variationally earlier.¹³ In order to improve the ground-state energy, we introduce an additional decaying parameter in the basis functions, and optimize the energy levels for a certain value of this parameter. With the decaying parameter we obtain the best variational estimate for the ground-state energy of -0.1257 for $N_{\text{basis}}=400$.

We show the first 20 eigenvalues obtained from different methods in Fig. 1 and the first five representative eigenvalues in Table II. As seen earlier, the real-space diagonalization

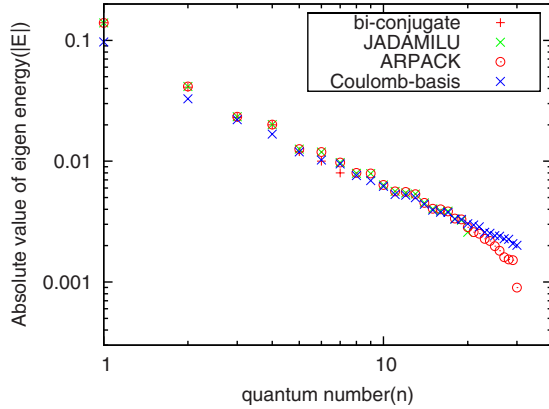


FIG. 1. (Color online) Comparison of eigenvalues obtained from different methods. (The plot is on a log-log scale.)

methods provide a better estimate of the ground-state energy whereas the Coulomb basis method is more suitable for higher excited states. The eigenvalues of both the Coulomb basis method and the real-space diagonalization methods are found to match each other for excited states and then they begin to deviate again (see Fig. 1). This can be understood by the fact that the extent of wave functions of the 2D edge-dislocation potential does not always increase as one goes to higher excited states—the wave functions of some excited states extend less than those of lower energy. Therefore, there are intermediate bound states that are missed in the real-space calculation because the size of grid used in calculation is not large enough to capture them. For example, we find four more bound states with the Coulomb basis calculation between the 18th and 19th excited states as calculated from the real-space diagonalization method. This feature also explains the abrupt increase in the eigenvalue of the 19th state calculated by using the Arnoldi-Lanczos method (ARPACK routine) in Fig. 1.

IV. SEMICLASSICAL ANALYSIS

It is usually insightful to consider the semiclassical solution of a quantum mechanics problem since the higher-energy eigenstates tend to approach classical behavior. A semiclassical estimate of the energy spectrum has been provided in Ref. 7. Here the total number of eigenstates up to a value of energy E is proportional to the volume occupied by

TABLE II. Comparison of first few energy eigenvalues obtained from different methods. Energy units: $2mp^2/\hbar^2$. n indicates quantum number of the state.

n	Biconjugate	Jacobi-Davidson/Arnoldi-Lanczos	Coulomb basis
1	-0.14	-0.139	-0.0970
2	-0.041	-0.0415	-0.0328
3	-0.023	-0.0233	-0.0221
4	-0.02	-0.0201	-0.0167
5	-0.012	-0.0126	-0.0119

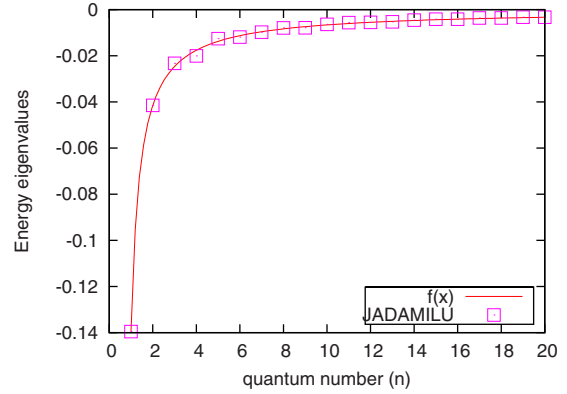


FIG. 2. (Color online) Fit for the eigenvalue spectrum obtained from JADAMILU using $f(x) = a(x-b)^c$. Fit values are -0.06, 0.61, and 0.96 for a , b , and c , respectively.

the system in the classical phase space. This is expressed by Weyl’s theorem,²³

$$n(E) = \frac{A}{4\pi} \frac{2m|E|}{\hbar^2} + \mathcal{O}\left(\sqrt{\frac{\hbar^2}{2mp^2}|E|}\right), \tag{9}$$

where A is the classically accessible area in real space and $|E|$ the absolute value of energy of the state. The higher-order corrections can be shown to be less important for higher excited states, which is where the semiclassical picture applies. To find A , we need the classical turning points for this potential determined by setting $E = V(r, \theta)$. Then the accessible area is the interior of a circle given by $(x - \frac{p}{2E})^2 + y^2 = (\frac{p}{2E})^2$ with area $A = \pi(p/2E)^2$. Therefore, we obtain (writing the nondimensionalized energy in our system of units as ϵ),

$$n(\epsilon) = -\frac{1}{16\epsilon}, \tag{10}$$

where n is the quantum number of the eigenstate and ϵ the corresponding energy. Note that the density of states $dn/d\epsilon$ scales as $1/\epsilon^2$.

To check this result we fit the numerical spectrum with the following functional form:

$$\epsilon(n) = a(n-b)^c \tag{11}$$

with the fitting parameters having values $a = -0.06$, $b = 0.5$, $c = -0.98$, each correct to within 5%. (Since we are dealing with bound states here, all the energy eigenvalues are negative, and the higher excited states have lower absolute eigenvalues.) We show the fit to the spectrum obtained from JADAMILU routine in Fig. 2. The semiclassically derived dependence is found to closely match with the fit for numerically calculated energy eigenstates, except for the $b = 0.5$ factor. In the limit of large n values, i.e., higher excited states, the fit relation tends to the semiclassical result as expected.

The classical trajectories for this potential bear the signature of chaotic dynamics showing space-filling nature and strong dependence on initial conditions. However, for reasons not yet clear to us, they are not ergodic, filling up only a wedge-shaped region in real space instead of the full

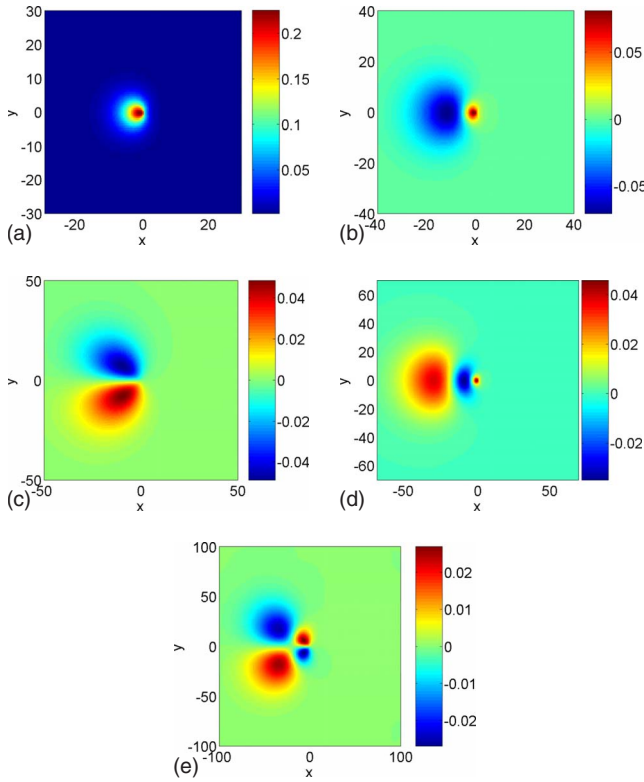


FIG. 3. (Color online) Eigenfunctions of the first five states. (a) ground state, (b) 1st excited state, (c) 2nd excited state, (d) 3rd excited state, and (e) 4th excited state. For clarity of presentation, the range of the x and y axes have been increased for the higher excited states.

classically allowed circle. The quantum mechanical probability density as calculated from the eigenfunctions also exhibits such wedge-shaped regions. Some sample wave functions obtained from our numerical calculations have been presented. Figure 3 shows the lowest five eigenstates and Fig. 4 shows some higher excited states. As expected, the wave functions are confined to the left half plane, where the potential is negative and bound states are possible. The parity of the potential shows up in the wave functions being either symmetric or antisymmetric about the x axis, although states of such “odd” and “even” parity do not always alternate. For example, the second and fourth excited states are odd, and the third excited state correspondingly even, but the ground state and first excited states are both even. Similarly the tenth, 50th, and 100th excited states are all odd while the 23rd and 24th are odd. The spatial extent of the wave functions is seen to be generally higher for higher excited states but this is not always the case. The extent does not scale monotonically with quantum number. Some cases are found where a higher excited state has less spatial extent than a lower one. For example we see in Fig. 4, that the 24th excited state is less extended in the x direction compared to the 23rd. We do not have any satisfactory explanation yet for these irregular features.

V. SUMMARY

In conclusion, we have investigated the long-standing quantum problem of a two-dimensional dipole potential. The

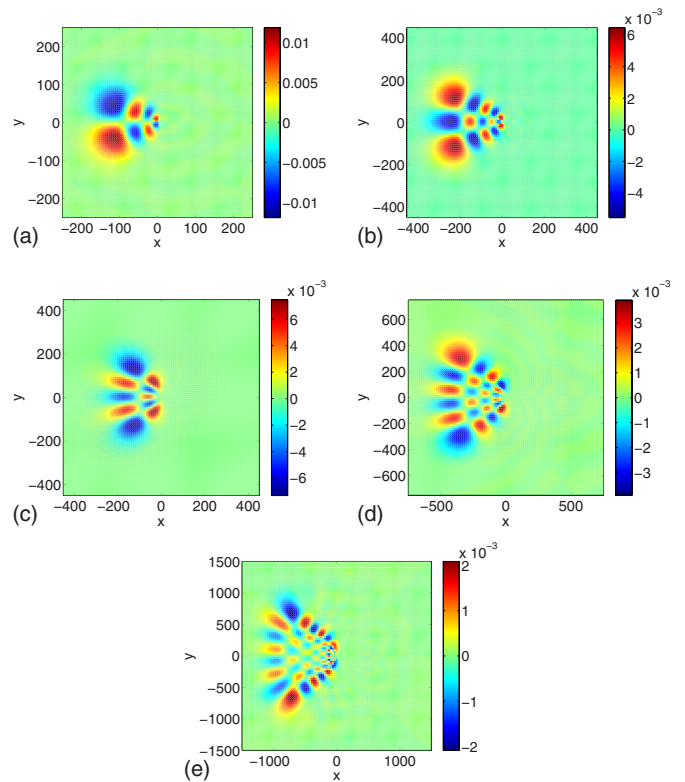


FIG. 4. (Color online) Eigenfunctions of five sample higher excited states. (a) 10th excited state, (b) 23rd excited state, (c) 24th excited state, (d) 50th excited state, and (e) 100th excited state. For clarity of presentation, the range of the x and y axes have been increased for the higher excited states.

wave functions and the spectrum are calculated by solving the Schrödinger equation with the 2D dipole potential numerically, and also, in the case of the ground state, variationally. We find that the results obtained from the different methods are consistent and compare favorably with previous estimates in the literature. We also discover a simple pattern in the spectrum, ($n \propto \epsilon^{-1}$), which can be justified from semiclassical considerations. Certain features of the spectrum and wave functions are yet to be explained and might provide scope for future investigation. For example, the statistics of the level spacings could possibly be a signature of quantum chaos. We hope to extend our work to studying dislocation-induced superfluidity as a model of ^4He supersolid.⁵ In such a model, the linearized GL equation is isomorphic to the Schrödinger equation, Eq. (2), and the ground-state energy and its wave function determined in this work provides an input to obtain the coupling constant g and the superfluid transition temperature modified by the presence of dislocations.

ACKNOWLEDGMENTS

We are grateful to H. B. Thacker for kindly providing us with a 2D Schrödinger equation solver based on the biconjugate gradient method, J. Toner for useful discussions and

ideas, C. Taylor for providing computational support, and S. Bera and A. Kemper for important suggestions regarding numerical methods. The authors acknowledge the University of Florida High-Performance Computing Center for provid-

ing computational resources and support that have contributed to the research results reported within this paper. This work was supported by NSF under Grant No. DMR-0705690.

-
- ¹A. H. Cottrell and M. A. Jaswon, *Proc. R. Soc. London, Ser. A* **199**, 104 (1949).
- ²A. Seeger, Day on Diffraction Millenium Workshop, International Seminar, 2000 (unpublished), p. 134.
- ³S. Balibar and F. Caupin, *J. Phys.: Condens. Matter* **20**, 173201 (2008).
- ⁴J. Toner, *Phys. Rev. Lett.* **100**, 035302 (2008).
- ⁵K. Dasbiswas, D. Goswami, C.-D. Yoo, and A. T. Dorsey (unpublished).
- ⁶R. Landauer, *Phys. Rev.* **94**, 1386 (1954).
- ⁷I. M. Lifshitz and K. I. Pushkarov, *JETP Lett.* **11**, 310 (1970).
- ⁸P. R. Emtage, *Phys. Rev.* **163**, 865 (1967).
- ⁹V. A. Slyusarev and K. A. Chishko, *Fiz. Met. Metalloved.* **58**, 877 (1984).
- ¹⁰I. M. Dubrovskii, *Low Temp. Phys.* **23**, 976 (1997).
- ¹¹V. M. Nabutovskii and B. Ya Shapiro, *JETP Lett.* **26**, 473 (1977).
- ¹²J.-L. Farvacque and P. Francois, *Phys. Status Solidi B* **223**, 635 (2001).
- ¹³A. T. Dorsey and J. Toner (unpublished), details are discussed in Sec. II of this paper.
- ¹⁴K. W. Morton and D. F. Mayers, *Numerical Solution of Partial Differential Equations, An Introduction* (Cambridge University Press, Cambridge, England, 2005).
- ¹⁵R. Fletcher, *Conjugate Gradient Methods for Indefinite Systems, Numerical Analysis* (Springer, New York, 1976), p. 73.
- ¹⁶G. L. G. Sleijpen and H. A. Van der Vorst, *SIAM J. Matrix Anal. Appl.* **17**, 401 (1996).
- ¹⁷C. Lanczos, *J. Res. Natl. Bur. Stand.* **45**, 255 (1950).
- ¹⁸M. Bollhöfer and Y. Notay, JADAMILU: software package based on Jacobi-Davidson method, available via <http://homepages.ulb.ac.be/~jadamilu/>, accessed on 4 July 2009.
- ¹⁹R. B. Lehoucq, D. C. Sorensen, and C. Yang, ARPACK: software package based on implicitly restarted Arnoldi methods, available via <http://www.caam.rice.edu/software/ARPACK/>, accessed on 4 July 2009.
- ²⁰M. Bollhöfer and Y. Notay, *Comput. Phys. Commun.* **177**, 951 (2007).
- ²¹R. B. Lehoucq, D. C. Sorensen, and C. Yang, *ARPACK Users' Guide: Solution of Large-Scale Eigenvalue Problems with Implicitly Restarted Arnoldi Methods* (SIAM, Philadelphia, PA, 1998).
- ²²X. L. Yang, S. H. Guo, F. T. Chan, K. W. Wong, and W. Y. Ching, *Phys. Rev. A* **43**, 1186 (1991).
- ²³M. C. Gutzwiller, *Chaos in Classical and Quantum Mechanics* (Springer-Verlag, New York, 1991).